1-O-acylceramides are natural components of human and mouse epidermis[S]

Mariona Rabionet,[*,†] **Aline Bayerle,**[*,†] **Christian Marsching,**[*,†,§] **Richard Jennemann,**[†] **Hermann-Josef Gröne,**[†] **Yildiz Yildiz,**[**] **Dagmar Wachten,**[††] **Walter Shaw,**[§§] **James A. Shayman,**[***] **and Roger Sandhoff**[1,*,†,§,†††]

Lipid Pathobiochemistry Group* within Department of Cellular and Molecular Pathology,[†] German Cancer Research Center (DKFZ), Heidelberg, Germany; Center for Applied Sciences at Technical Universities (ZAFH)-Applied Biomedical Mass Spectrometry (ABIMAS),[§] Mannheim, Germany; Innere Medizin am Landeskrankenhaus Bregenz,[**] Bregenz, Austria; Department of Molecular Sensory Systems,[††] Molecular Physiology Group, Center of Advanced European Studies and Research (CAESAR), Bonn, Germany; Avanti Polar Lipids, Inc.,[§§] Alabaster, AL; Nephrology Division,[***] Department of Internal Medicine, University of Michigan, Ann Arbor, MI; and Instrumental Analytics and Bioanalytics,[†††] Technical University of Applied Sciences, Mannheim, Germany

Abstract The lipid-rich stratum corneum functions as a barrier against pathogens and desiccation inter alia by an unbroken meshwork of extracellular lipid lamellae. These lamellae are composed of cholesterol, fatty acids, and ceramides (Cers) in an equimolar ratio. The huge class of skin Cers consists of three groups: group I, "classical" long and very long chain Cers; group II, ultra-long chain Cers; and group III, ω-esterified ultra-long chain Cers, which are esterified either with linoleic acid or with cornified envelope proteins and are required for the water permeability barrier. Here, we describe 1-O-acylceramides as a new class of epidermal Cers in humans and mice. These Cers contain, in both the N- and 1-O-position, long to very long acyl chains. They derive from the group I of classical Cers and make up 5% of all esterified Cers. Considering their chemical structure and hydrophobicity, we presume 1-O-acylceramides to contribute to the water barrier homeostasis. Biosynthesis of 1-O-acylceramides is not dependent on lysosomal phospholipase A_2. However, glucosylceramide synthase deficiency was followed by a 7-fold increase of 1-O-acylceramides, which then contributed 30% to all esterified Cers. Furthermore, loss of neutral glucosylceramidase resulted in decreased levels of a 1-O-acylceramide subgroup.[S] Therefore, we propose 1-O-acylceramides to be synthesized at endoplasmic reticulum-related sites.—Rabionet, M., A. Bayerle, C. Marsching, R. Jennemann, H-J. Gröne, Y. Yildiz, D. Wachten, W. Shaw, J. A. Shayman, and R. Sandhoff. **1-O-acylceramides are natural components of human and mouse epidermis.** *J. Lipid Res.* **2013.** 54: 3312–3321.

Supplementary key words ceramide • stratum corneum • skin • UDP-glucose ceramide glucosyltransferase • glucosidase beta 2 • lysosomal phospholipase A_2 • omega-esterified

Ceramides (Cers) are bioactive membrane lipids involved in a great variety of key cellular functions, including the control of cellular fate in programmed cell death (1, 2). In sphingolipid pathways Cers reflect a branching point. Either their degradation leads to free sphingoid bases and further to sphingosine-1-phosphates, which function as signaling molecules promoting cell survival (3), or they may be used as building blocks for membrane lipids, i.e., sphingomyelins (SMs), galactosylceramides, and glucosylceramides (GlcCers). Further glycosylation of GlcCers leads to the formation of hundreds of more complex glycosphingolipids (GSLs) (4). Finally, Cers may also be phosphorylated directly and the resulting ceramide-1-phosphate stimulates group IVA cytosolic phospholipase $A_2\alpha$ to release arachidonic acid from phosphatidylcholines leading to the vast class of signaling eicosanoids (5–7) (**Fig. 1**).

The outermost layer of mammalian skin, the epidermis, is rich in Cers needed for proper skin barrier functions (8, 9). Epidermal Cers are mainly found in extracellular

---

Abbreviations: Cer, ceramide; CerS3, ceramide synthase 3; Dga1p, diacylglycerol O-acyltransferase, DGAT2, diacylglycerol O-acyltransferase 2; EOS, esterified ω-hydroxyceramides with a sphingosine backbone; ER, endoplasmic reticulum; Gba2, glucosidase beta 2, also non-lysosomal/neutral glucosylceramidase; GlcCer, glucosylceramide; GlcCer-S, glucosylceramide synthase; GSL, glycosphingolipid; K14, keratin 14 (also KRT14); LPLA$_2$, group XV lysosomal phospholipase A_2 (PLA2G15); Lro1p, phospholipid:diacylglycerol acyltransferase; NS-Cer, non-hydroxyfatty acid and sphingosine containing ceramides; P, post natal day; POS, protein bound ceramides with a sphingosine backbone; RP, reversed-phase; SRM, single reaction monitoring; Ugcg, UDP-glucose ceramide glucosyltransferase or glucosylceramide synthase; UPLC-ESI-MS/MS, ultra performance liquid chromatography coupled-electrospray ionization-tandem mass spectrometry.

[1]To whom correspondence should be addressed.
  e-mail: r.sandhoff@dkfz.de or r.sandhoff@hs-mannheim.de
[S] The online version of this article (available at http://www.jlr.org) contains supplementary data in the form of text, seven figures, and two tables.

lipid lamellae surrounding corneocytes of the stratum corneum. Here, special Cer structures with amide-bond ultra-long[2] chain ω-hydroxylated fatty acids exist that are formed by ceramide synthase 3 (CerS3) (10) (Fig. 1). This ω-hydroxylation is a prerequisite for further esterification of Cers with long chain fatty acids, predominantly linoleic acid ($\Delta^{9,12}$-18:2), or esterification with proteins of the cornified envelope, as reviewed in (11–15). Although esterified Cers gain hydrophobicity due to their ultra-long chain fatty acid and esterification in the ω-position, they retain their polar head group structure with two hydroxy groups (three hydroxy groups in phyto-compounds).

An alternative metabolic pathway for Cers was suggested first in the late seventies, when tissue or cells were shown to esterify labeled Cers in 1-O-position of the sphingoid base. Injection of ^{3}H- and ^{14}C-labeled Cers (d18:1;16:0 and d18:1;24:0)[3] directly into rat brains led, among other products, to 1-O-acylceramides (16). Subsequently, a group XV lysosomal phospholipase A$_2$ (LPLA$_2$) was discovered with the unique ability to transacylate in vitro radioactive short chain Cers in 1-O-position (17), reviewed in (18). Recently, a pathway leading to 1-O-acylceramides was described in yeast. It involves the diacylglycerol acyltransferases phospholipid:diacylglycerol acyltransferase (Lro1p) and diacylglycerol O-acyltransferase (Dga1p), which in contrast to the LPLA$_2$ also esterified very long chain Cers in 1-O-position (19). Here, we report the identification and structural characterization of natural 1-O-acylceramides in mouse and human epidermis. Using ultra performance liquid chromatography coupled-electrospray ionization-tandem mass spectrometry (UPLC-ESI-MS/MS), we identified and quantified a group of almost 100 species in mice. Combinatorial calculations suggest the presence of more than 200 subspecies in mouse epidermis. To our knowledge, this study is the first description of endogenously expressed 1-O-acylceramides in mammals.

MATERIALS AND METHODS

Materials

Epidermal lipid extracts of glucosidase beta 2 (Gba2, nGlcCerase)-, LPLA$_2$-, glucosylceramide synthase (GlcCer-S)-, and CerS3-deficient mice were used for mass spectrometric analyses.

---

[2] Long chain fatty acids or Cers are defined here as those with an acyl moiety ranging from 16 to 20 carbon atoms, very long chain as those with 22 to 26 carbon atoms, and ultra-long chain as those with 28 or more carbon atoms.

[3] Cers are structurally described according to their sphingoid base and fatty acid moieties. In brackets, first is described the type of sphingoid base. The initial letter refers to the number of hydroxy groups (m, mono; d, di; t, tri; or te, tetra), the following number corresponds to the amount of carbons of the linear chain and the number after the colon corresponds to the degree of unsaturation. After the semicolon, the fatty acid in 2-N-position is described first with the number of carbons in the acyl chain and after the colon the number of unsaturations. If the fatty acid is hydroxylated, an "h" is placed in front of the number of carbons or "ω" when hydroxylation occurs at ω-position. Specifically for 1-O-acylceramides we included the description of the fatty acid attached in 1-O-position (including number of carbons and hydroxylation) prior to the specification of their sphingoid base.

nGlcCerase-deficient mice lack the neutral glucosylceramidase, which may lead to increased nonlysosomal GlcCer levels, and by that may potentially lead to decreased Cer levels as substrate for 1-O-acylation. LPLA$_2$-deficient mice lack LPLA$_2$, which was reported to have 1-O-acylating activity on short chain Cers. Hence, it could have been a candidate for 1-O-acylation of Cers in epidermis. Lipid extracts from nGlcCerase- and LPLA$_2$-mutants were obtained from the mouse lines published in (20, 21). Mice with epidermal deficiency of UDP-glucose ceramide glucosyltransferase (*Ugcg*) lack GlcCer-S in epidermal keratinocytes. Epidermal lipid extracts of *Ugcg*-keratin 14 (K14) mice were from (22). CerS3 is essential for the synthesis of Cers containing *N*-linked ultra-long chain fatty acids, which are abundantly expressed in epidermis. Lipid extracts used were from CerS3-mice, recently published (10), and lack ω-esterified Cers.

For mass spectrometric analyses the following internal standards were used. Standard 1: 1-*O*-oleoyl-*N*-heptadecanoyl-*D*-erythro-C18-sphingosine, Cer(18:1;d18:1;17:0); and standard 2: 1-*O*-palmitoyl-*N*-palmitoyl-*D*-erythro-C18-sphingosine, Cer(16:0;d18:1;16:0) were obtained from Avanti Polar Lipids Inc., Alabaster, AL. For quantification of classical Cers and GlcCers, the following chemically-synthesized internal standards were used: Cer(d18:1;14:0), Cer(d18:1;19:0), Cer(d18:1;25:0), Cer(d18:1;31:0), GlcCer(d18:1;14:0), GlcCer(d18:1;19:0), GlcCer(d18:1;25:0), and GlcCer(d18:1;31:0) (22).

Samples were extracted with solvents of per analysis grade. For UPLC-ESI-MS/MS analysis, dried aliquots were taken up in solvents used for chromatography which were of HPLC grade. All additives used were also of HPLC grade.

The adhesive tape (tesa® film transparent, #57371) used for lipid isolation of human stratum corneum was composed of polypropylene with an acrylic adhesive.

Preparation of epidermis and isolation of epidermal lipids

Epidermis was separated from dermis and raw extracts of epidermal lipids were prepared according to (10). In brief, interscapular skin samples were rapidly dissected and snap-frozen. To separate epidermis from dermis, samples were treated with 500 mg/ml thermolysin buffer (containing 10 mM 4-(2-hydroxyethyl)-1-piperazineethanesulfonic acid (HEPES), 142 mM NaCl, 6.7 mM KCl, 0.43 mM NaOH, and 1 mM CaCl$_2$ at pH 7.4) for 2 h at 37°C. Isolated epidermis was cut into small pieces and lyophilized. Roughly 3 mg of dry weight epidermis was extracted with 2 ml of chloroform/methanol/water (30/60/8) by volume at 50°C for 15 min under sonication. Supernatant was taken after centrifugation and pellets were reextracted two additional times using the solvent mixtures of chloroform/methanol/distilled water (10/10/1) and chloroform/methanol (2/1) by volume. Supernatants were pooled and desalted using reversed-phase (RP)-18 columns.

Internal standards were added to aliquots of the lipid extracts prior to being analyzed by UPLC-ESI-MS/MS. Aliquots of lipid extracts from Ugcg-K14 mice were taken from the samples prepared for the publication of (22).

Isolation of human stratum corneum lipids

Isolation of human stratum corneum was performed by tape stripping in healthy male volunteers with ages ranging from 26 to 45 years. The volunteers were asked not to apply any cosmetic skin products on their ventral forearms within 16 h prior to sample collection. The human studies were approved by the ethics committee of the Medical Faculty, University of Heidelberg, Germany and informed consent of participants was obtained.

Both ventral forearms of each volunteer were stripped in four consecutive sites using ordinary adhesive tape in an area of 2 ×
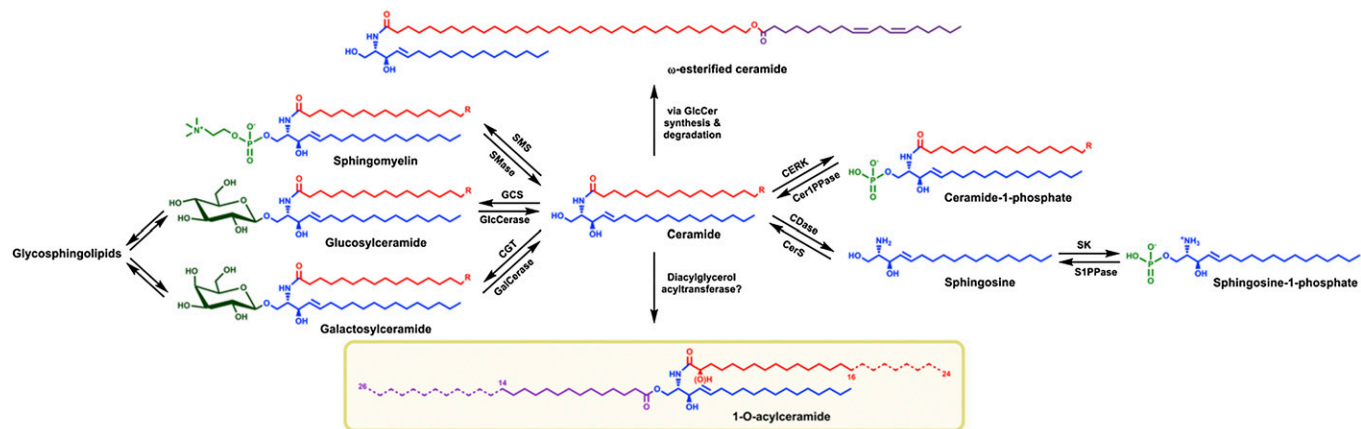
Fig. 1. General Cer metabolism. Cers reside at the epicenter of the sphingolipid metabolism. They can be converted into ubiquitously expressed SMs and GSLs. However, the glycan pattern of GSLs found is cell type specific, e.g., galactosylceramide synthesis is mainly restricted to myelin sheaths, renal tubular epithelial cells, and pancreatic islets, but is not present in the epidermis. Cers are also precursors of the bioactive lipids ceramide-1-phosphate and, via sphingosines, of sphingosine-1-phosphate. In the epidermis, Cers with ultra-long ω-hydroxy acyl chains are further ω-esterified, mainly with linoleic acid. These ω-esterified Cers are imperative for adequate skin barrier functions. Reported here, epidermal Cers with N-linked long and very long chain fatty acids (C16–C24) may also be esterified with saturated long and very long chain fatty acids (C14–C26) in 1-O-position leading to 1-O-acylceramides.

1.5 cm. For each stripping, tapes were pressed with a weight of 4.8 kg for 30 s prior to being peeled off with tweezers in a single sharp stroke. Tape strips were individually placed in glass vials and were extracted with 3.5 ml chloroform/methanol/water (30/60/8) for 15 min at 37°C with a subsequent centrifugation step for 10 min at 3,500 g. An aliquot (3 ml) of each of the four extracts containing the lipids of the consecutive tape strips of one forearm of each volunteer were pooled and dried. Thus, duplicates of three volunteers were processed. Extracts were then redissolved in methanol/water (95/5, 2 ml) and centrifuged for 15 min at 21,000 g. Internal standards were added to a final aliquot of the extracts (1 ml) prior to be quantified by UPLC-ESI-MS/MS. The standards used were as follows: for 1-O-acylceramides, Cer(18:1;d18:1;17:0); for classical Cers, Cer(d18:1;14:0), Cer(d18:1;19:0), Cer(d18:1;25:0), and Cer(d18:1;31:0). To exclude contaminations or artifacts from the adhesive tape, the latter was used as a blank and extracted in parallel with the human probes. Aliquots were analyzed by UPLC-ESI-MS/MS for 1-O-acylceramides, as well as classical non-hydroxyfatty acid and sphingosine containing ceramides (NS-Cers), with acyl chains from 16 to 36 carbon atoms and a C18-sphingosine base. The amount of 1-O-acylceramides in fmol was normalized to the total amount of NS-Cers in pmol.

Lipid analysis by UPLC-ESI-MS/MS

UPLC-ESI-(triple quadrupole)MS/MS analysis was performed on a Xevo TQ-S tandem mass spectrometer coupled to an automated Aquity I class UPLC system using an ACQUITY UPLC® BEH C18 1.7 μm column (length 50 mm, diameter 2.1 mm) all from Waters Corporation. The column was equilibrated in buffer A (95% methanol, 0.05% formic acid, and 1 mM ammonium formate) and lipids were eluted with increasing percent of buffer B (99% 2-propanol, 1% methanol, 0.05% formic acid, and 1 mM ammonium formate) at a flow rate of 0.45 ml/min as described in (23) with slight modifications as follows: The gradient went up to 90% B as listed in supplementary Table I. The total gradient time was fixed at 6.5 min per run. As previously, samples were dissolved in 95% methanol and 5% water. However, care was taken that samples were treated in an ultrasound bath for 3 min at 40°C and then placed directly into the auto sampler, which was held at 20°C. The column was heated to 40°C and in general 10 μl (100% of injection needle capacity) aliquots were injected.

Protonated 1-O-acylceramides were quantified in single reaction monitoring (SRM) mode using 7.65 pmol of 1-O-oleoyl Cer(d18:1;17:0) as internal standard per aliquot of epidermal lipids corresponding either to 0.1 mg mouse tissue dry weight or to 5.1 cm^2 of tape used for stripping human stratum corneum. The capillary voltage was set at 2.5 kV, whereas the cone and the source offset were fixed at 50 V. The source and desolvation temperatures were maintained at 90 and 300°C, respectively. The desolvation gas was delivered at 800 l/h, while the cone gas and the collision gas flow were fixed at 150 l/h and 0.15 ml/min, respectively. 1-O-acylceramides were detected using a fixed collision energy of 20 eV, while maintaining the dwell time at 8 ms. Instead classical Cers (d18:1;14:0–36:0) were measured using increasing collision energies ranging from 25 to 30 eV according to their molecular mass.

Significant in-source decay of 1-O-acylceramides leading to water loss appeared. Therefore, each compound was detected by two transitions, which were added up for quantification: *i*) transition of the protonated acylceramide to fragment C (loss of a water molecule and the O-linked fatty acid); and *ii*) transition of the mono-dehydrated and protonated acylceramide to fragment C. The decision basis for the incorporation of individual acylceramides into the final multiple reaction monitoring list (supplementary Table II) was based on precursor ion scan m/z +264 mode by which all potential acylceramides with a C18-sphingosine (d18:1) were detected.

Samples were injected and processed using MassLynx, whereas mass spectrometric peaks were quantified according to their peak area ratio with respect to the internal standard using TargetLynx (both v 4.1 SCN 843) both from Waters Corporation.

Validation of the method: linearity assay and matrix effects evaluation

Linearity of the method was analyzed keeping the amount of internal standard 1 constant at 7.65 pmol while diluting several times by 1:2 the amount of standard 2, 1-O-palmitoyl Cer(d18:1;16:0). Linearity of the method was obtained down to 8.8 fmol of 1-O-palmitoyl Cer(d18:1;16:0) with 10% deviation from the regression curve (supplementary Fig. IA). In a second experiment, the amount of murine epidermal lipid extract was diluted against a constant concentration of 7.65 pmol of internal standard, and the series of 1-O-acylceramides with the very long chain Cer

anchor Cer(d18:1;24:0) was quantified. The obtained curve demonstrates the amount of lipid extract corresponding to 0.1 mg tissue dry weight within the linear range (supplementary Fig. IB).

To evaluate matrix effects from the adhesive tape in human epidermal extracts, a dilution of 1-O-palmitoyl Cer(d18:1;16:0) with a fixed amount of 7.65 pmol internal standard was evaluated in the absence and presence of blank tape extracts obtained according to the method described for the isolation of human stratum corneum lipids (supplementary Fig. IC).

RESULTS

Alkaline sensitive Cers of unknown composition in mouse epidermis

Screening total epidermal lipid extracts for Cers containing a C18-sphingosine base (d18:1) by MS/MS, we detected low abundant signals for compounds with an even protonated nominal mass in the range of m/z 750–1,000 (supplementary Fig. II). These signals did not fit to any previously known epidermal Cers and GlcCers or ultra-long chain ω-esterified Cers. Furthermore, these signals were present not only in samples of wild-type mice, but also in samples of CerS3-deficient mice [lacking ultra-long chain and

ω-esterified Cers (10)], and in samples of GlcCer-synthase-deficient (keratinocyte-specific) mice, which do not contain epidermal GlcCers (22). Hence, the unidentified peaks neither belonged to GlcCers nor to Cers with ultra-long chain Cer anchors. The lipids underlying these signals were sensitive to alkaline treatment and appeared enriched in lipid extracts of GSL-free epidermis, i.e., from keratinocyte-specific GlcCer-synthase-deficient mice. Simultaneously, alkaline treatment increased the amount of long and very long chain (C16–C24) Cers in wild-type but especially in GSL-free epidermis. Therefore, we hypothesized the unknown lipids to be alkaline-sensitive derivatives of long and very long chain Cers, e.g., esterified Cers. Product ion spectra from the main peaks indeed revealed fragmentation patterns that included a parent Cer backbone: all fragmentation spectra contained three dominant product ions due to: *i*) loss of a water molecule, *ii*) loss of a water molecule and lignoceric acid, and *iii*) a residual dehydrated d18:1-sphingosine base (**Fig. 2**, product ions in red small letters a, c, and e).

Subgroups of O-acylceramides identified by specific product ion and retention time

In a next step, we performed precursor ion screens of the epidermal lipid extract using the c-type fragments,
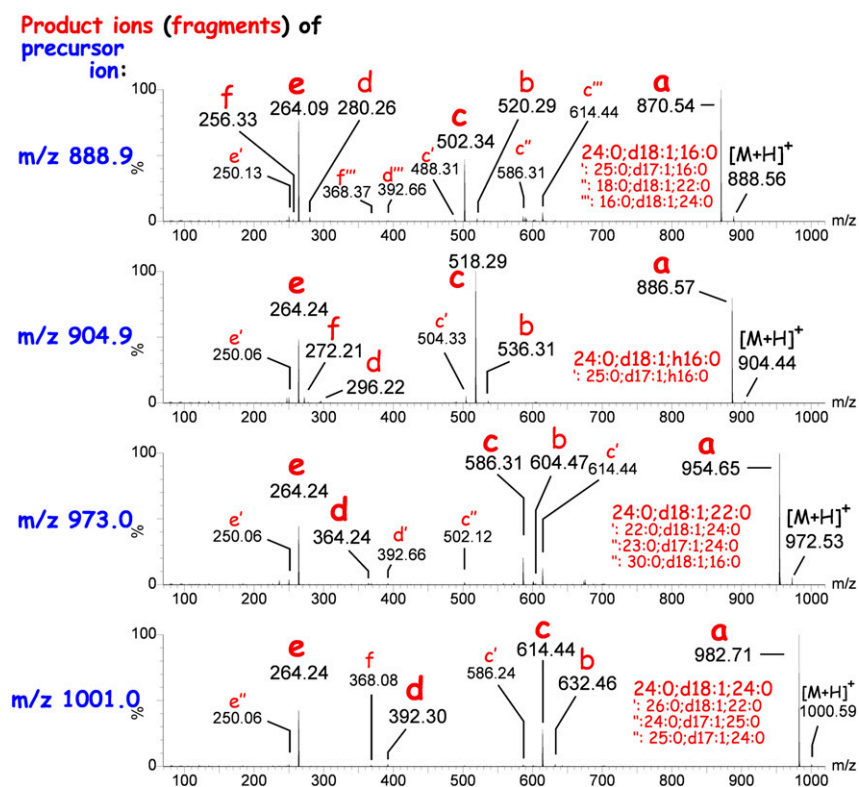

Fig. 2. Tandem mass spectrometric fingerprint of selected unknown Cers. CerS3-deficient epidermal lipid extracts were injected on a RP-18 column and eluting compounds were monitored in product ion mode set to the corresponding m/z values of unknown Cers. Product ion spectra (0.2 s/spectrum) corresponding to the complete peak width (5–6 s, i.e., 25–30 spectra) of the eluting unknown Cer species (see Fig. 3) were summed up into each spectrum plotted here. In the product ion mode, molecular ions (precursor ions, blue m/z) of unknown Cers were fragmented within the mass spectrometer by collision-induced dissociation to generate characteristic product ions (red small letters). Main fragments are annotated in bold letters and the corresponding acylceramide composition is written in larger letters on top. Alternative fragments and corresponding minor acylceramides coeluting within the same UPLC-peak are annotated in small letters with primes. Small red letters denote specific types of fragments described in the scheme of Fig. 4.

which might correspond to doubly dehydrated Cer backbones. To exclude an involvement of known ω-esterified ultra-long chain Cers, we used an extract of CerS3-deficient mice, that lack Cers with fatty acids greater than lignoceric acid (10). For each c-type fragment scan, we identified a series of lipids fitting to the esterification of the corresponding Cer backbone with long to very long chain saturated fatty acids (supplementary Fig. II).

Using the information of the precursor ion scans, we established a SRM-based RP-18 chromatography for a more specific and sensitive detection of 1-O-acylceramides (**Fig. 3**). Using the transition of the molecular ions to their c-type fragment (see scheme of **Fig. 4A**), which is specific for the parent Cer backbone, characteristic elution times of individual acylceramides were obtained that depended on the length of the acyl chain in ester linkage. Likewise, by keeping the 1-O-acyl chain constant the retention times increased with increasing size of the Cer backbone (Fig. 3B vertical lines).

The characteristic retention time curves (Fig. 3B) allowed predictions with regard to the O-acyl chain length of 1-O-acylceramides. Interestingly, structurally isomeric 1-O-acylceramides eluted simultaneously and could only be

differentiated by the SRMs used (Fig. 3B, horizontal line); e.g., 1-O-lignoceroyl-Cer(d18:1;16:0) (Fig. 3A, series 16, peak I) and 1-O-palmitoyl Cer(d18:1;24:0) (Fig. 3A, series 24, peak C) eluted simultaneously, but differed in their SRM by the transition to m/z 502 and 614, respectively.

We then compared the retention times of 1-O-acylceramides with those of linoleic acid esterified ω-hydroxyceramides (EOS-Cers). Whereas 1-O-acylated long chain Cers eluted earlier than EOS-Cers, 1-O-acylated very long chain Cers had a similar or even higher retention time than EOS-Cers on the RP-18 column. The additional free hydroxy group in 1-position and the two double bonds of the linoleic acid reduced the interaction with the RP-18 column so that EOS-Cers eluted much earlier than the corresponding 1-O-acylceramides with the same total amount of carbon atoms. For example, EOS-Cer(d18:1;30:0;ω18:2) eluted 0.4 min earlier than 1-O-acylceramide (24:0;d18:1;24:0), both having in total 66 carbon atoms. EOS-ceramides with a saturated ultra-long chain omega-hydroxy fatty acid needed roughly 7 to 8 more CH_2-units to reach the same hydrophobicity than corresponding 1-O-acylceramides on the RP-18 column (supplementary Fig. III).
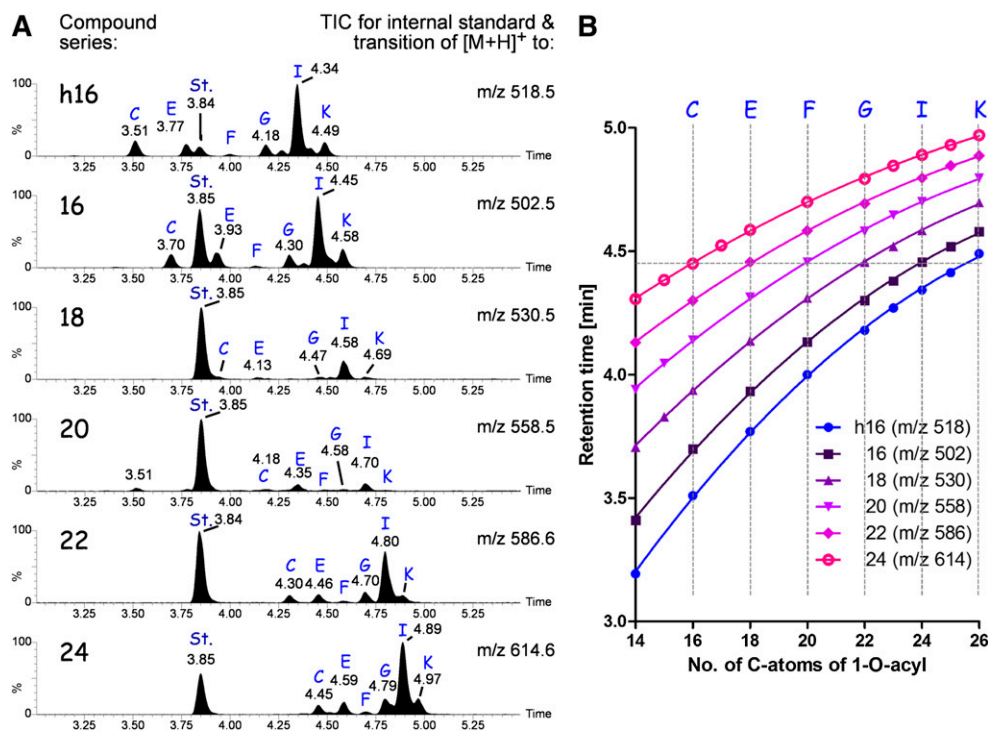

Fig. 3. RP chromatography of 1-O-acylceramides. 1-O-acylceramide (with a C18-sphingosine, d18:1) were recorded in subseries according to the parent Cers they derived from [h16, Cer(d18:1;h16:0); 16, Cer(d18:1;16:0); 18, Cer(d18:1;18:0); 20, Cer(d18:20:0); 22, Cer(d18:22:0); and 24, Cer(d18:24:0)]. To exclude interference with ω-esterified Cers, epidermal lipid extracts from CerS3-deficient mice were used. A: Total ion chromatogram of the subseries of 1-O-acylceramides. Lipids were separated using a RP-18 column. Blue capital letters depict peaks of acylceramides with defined 1-O-acyl chain: C, C16:0; E, C18:0; F, C20:0; G, C22:0; I, C24:0; and K, C26:0. Other species recorded either appear in between these peaks and are not annotated, e.g., H, C23:0, or are observed in respective extracted ion chromatograms (not shown), but their concentration is too low to be observed in total ion chromatograms, e.g., A, 14:0. St. denotes the internal standard 1-O-oleoyl Cer(d18:1;17:0) measured with the transition to m/z 516. B: Retention times of 1-O-acylceramides on RP-18 column are plotted in dependence of the saturated acyl chain in ester linkage for the different parent Cer backbones. Data points are the mean ± standard deviation (SD ≤ 0.01 min) of three different biological samples. Curves were obtained by nonlinear regression (second order polynomial). For all curves, $R^2 ≥ 0.999$.
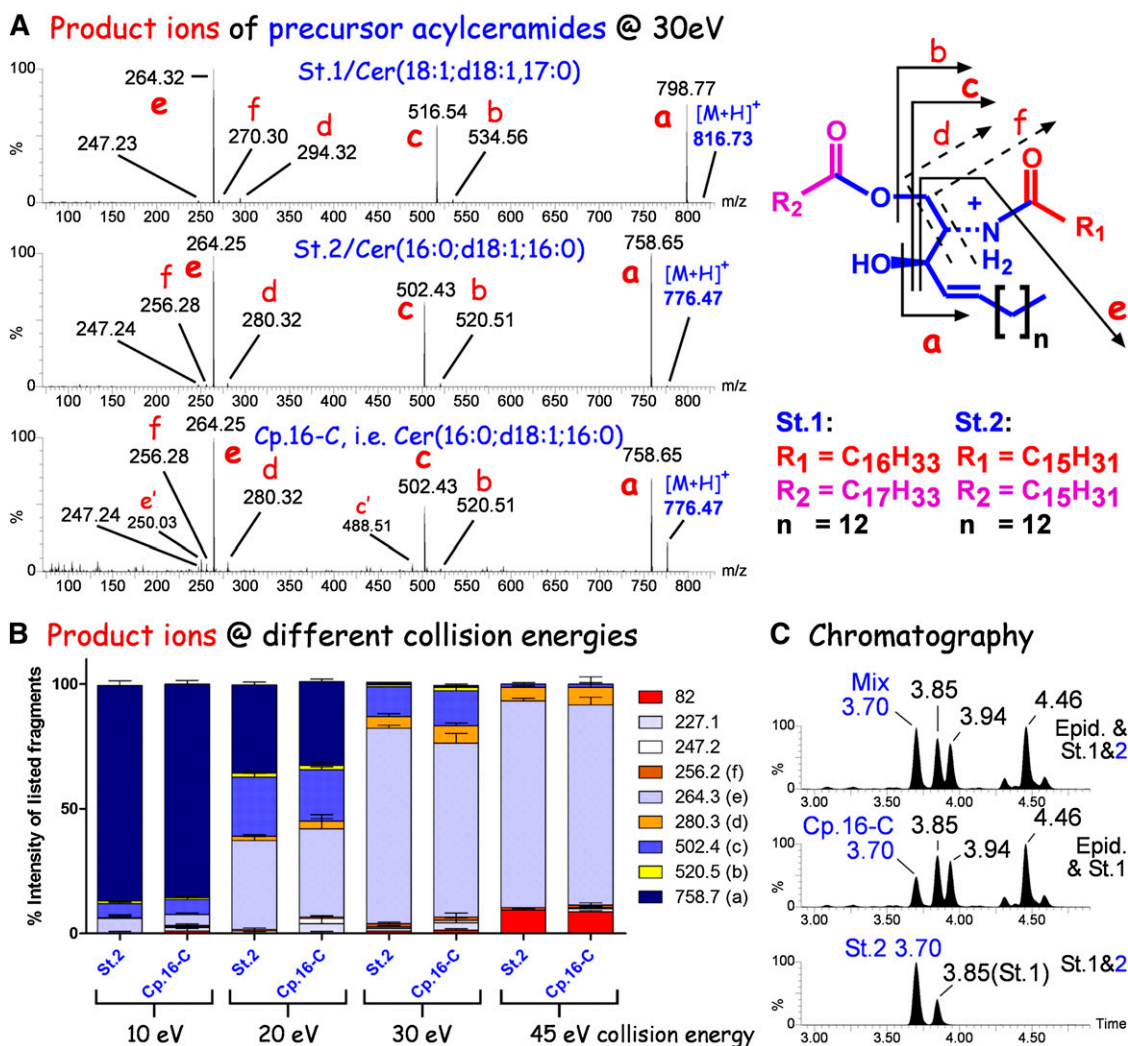
Fig. 4. Mass spectrometric and chromatographic comparison of synthetic and epidermis-derived 1-O-acylceramides. Chemically synthesized standard 2 (St.2), 1-O-palmitoyl-N-palmitoyl C18-sphingosine [Cer(16:0;d18:1;16:0)] was compared with the epidermis-derived acylceramide annotated in series 16 of Fig. 3 as peak (compound) "C" (Cp.16-C). A: Product ion spectra of protonated 1-O-acylceramides ([M+H]⁺), standard 1 (St.1), 1-O-oleoyl,N-heptadecanoyl C18-sphingosine/Cer(18:1;d18:1;17:0); standard 2 (St.2), 1-O-palmitoyl,N-palmitoyl C18-sphingosine/Cer(16:0;d18:1;16:0); Cp.16-C, acylceramide "C" of series 16 (see Fig. 3) from epidermal lipid extract of CerS3-deficient mice. Average product ion spectra were recorded from the chromatographic peaks as described in the Fig. 2 legend. The scheme on the right illustrates the structure of 1-O-acylceramides and the product ions (derived by collision-induced dissociation) annotated with small red letters within the spectra. Letters with a prime mark fragments from other minor acylceramides of the same nominal mass coeluting with endogenous Cp.16-C, i.e., Cer(16:0;d18:1;16:0). B: Comparison of product ion peaks in standard 2 [Cer(16:0;d18:1;16:0)] and acylceramide Cp.16-C from CerS3-deficient epidermis recorded at different collision energies. Chromatograms were recorded in product ion mode. Product ion spectra of the complete peak at 3.7 min (see Fig. 4C) were summed up to produce an average spectrum for evaluation. Note the identical product ion ratios from both samples at all collision energies investigated for all fragments (82.0–758.7). C: Bottom spectrum: mixture of the synthetic standards, Cer(16:0;d18:1;16:0) and Cer(18:1;d18:0;17:0); middle spectrum: raw lipid extract from mouse epidermis; upper spectrum: mixture of epidermal sample as seen in middle spectrum with standard Cer(16:0;d18:1;16:0). Note, the mixture contains a single peak at 3.7 min supporting further the identity of the synthetic standard and the endogenous compound.

Identification as 1-O-acylceramides

To identify the epidermal acylceramides as 1-O-acylceramides, we compared the retention times and fragmentation patterns of the endogenous compounds with synthetic 1-O-acylceramide standards. Comparing the fragmentation behavior of the two standard compounds, 1-O-palmitoyl Cer(d18:1;16:0) and 1-O-oleoyl Cer(d18:1;17:0), we could attribute the individual product ions to the Cer backbone (fragments b and c, Fig. 4A), the sphingoid base (fragment e, Fig. 4A), and to ions containing the amide bond acyl chain (fragments d and f, Fig. 4A). No specific product ions

for the 1-O-acyl chain were obtained. The O-acyl chain rather gave rise to a neutral loss (Fig. 4A). The product ion spectra of 1-O-palmitoyl Cer(d18:1;16:0) and the corresponding endogenous compound were not only identical at a collision energy of 20 eV (Fig. 4A, B), but also at 10, 30, and 45 eV with respect to the relative intensities of their fragment ions to each other (Fig. 4B). Furthermore, the synthesized compound eluted identical to the respective endogenous compound (t_R = 3.70 min, Fig. 4C; see also Fig. 3, series 16). Thus, we concluded that the detected acylceramides of mouse epidermis represent 1-O-acylceramides.

Quantification reveals 1-O-acylceramides are a minor group of esterified Cers in wild-type mouse epidermis

We investigated epidermal lipid extracts from wild-type and mutant mice of a mouse strain with a constitutive cell-specific deficiency of GlcCer-S (gene, *Ugcg*) in K14 expressing cells (basal keratinocytes) 4 days after birth. From this strain we had previously published the Cer, glucosylceramide, and SM levels in epidermis at this age. The mutant mice do not synthesize GlcCers in epidermal keratinocytes anymore and have a deficient water permeability barrier (22).

In GlcCer-S wild-type mice we identified 248 ± 53 pmol 1-O-acylceramides containing a C18-sphingosine and 155 ± 31 pmol 1-O-acylceramides containing a C17-sphingosine. A comparison with the published (18) total amount of ω-esterified C18-sphingosine base-containing Cers [EOS + protein bound ceramides with a sphingosine backbone (POS)] revealed C18-sphingosine base containing 1-O-acylceramides to make up 4.6% of all esterified Cers (sum of EOS-, POS-, and 1-O-acylceramides with a C18-sphingosine base) or 4.3% of all esterified sphingolipids (including esterified GlcCers and SMs with a C18-sphingosine base) in epidermis of 4-day-old GlcCer-S wild-type mice.

Transacylation and 1-O-glucosylation seem to compete for Cer as substrate

Acylation of Cers in 1-O-position makes it impossible for Cer to be transformed into GSLs through either 1-O-galactosylation or 1-O-glucosylation, or into SM. To investigate whether these pathways compete with each other, we analyzed the epidermis of mice deficient in GlcCer synthesis. In fact, the sum of 1-O-acylceramides increased about 7-fold in

4-day-old mutant mice (**Fig. 5**). While Cers with a 1-O-very long chain fatty acid ester, e.g., 1-O-lignoceroyl Cers, increased only 3- to 4-fold, 1-O-palmitoyl and 1-O-stearoyl Cers increased 60- and 80-fold, respectively (supplementary Fig. IV). In the epidermis of GlcCer-S-deficient mice, 1-O-acylceramides increased to 31% of all esterified Cers (31% of all esterified sphingolipids) or to 16% of all sphingolipids, when comparing data obtained here with the previously published data (22) on the basis of C18-sphingosine-containing sphingolipids. Hence, Cers not transformed into GlcCer may further on be converted into 1-O-acylceramides.

We compared the quantities of 1-O-acylceramides with those of the corresponding unmodified parent Cers obtained before and after mild saponification, as the increase of parent Cers after saponification should reflect mild alkaline-sensitive Cer esters. These data had been obtained previously with a MS/MS instrument only (22). Indeed, the total amount of these parent Cers increased significantly after saponification in both control and GlcCer-S-deficient epidermis. Furthermore, the difference in amounts reflecting mild alkaline-sensitive derivates of these Cers correlated quite well the amounts of 1-O-acylceramides determined now by UPLC-MS/MS (supplementary Fig. V). While in wild-type epidermis one out of six parent Cers was found to be 1-O-esterified, in GlcCer-S-deficient epidermis every second parent Cer was 1-O-acylated.

Epidermal 1-O-acylceramide synthesis occurs in the absence of LPLA$_2$

LPLA$_2$ contains transacylation activity and has been shown to produce 1-O-acylceramides, especially using short
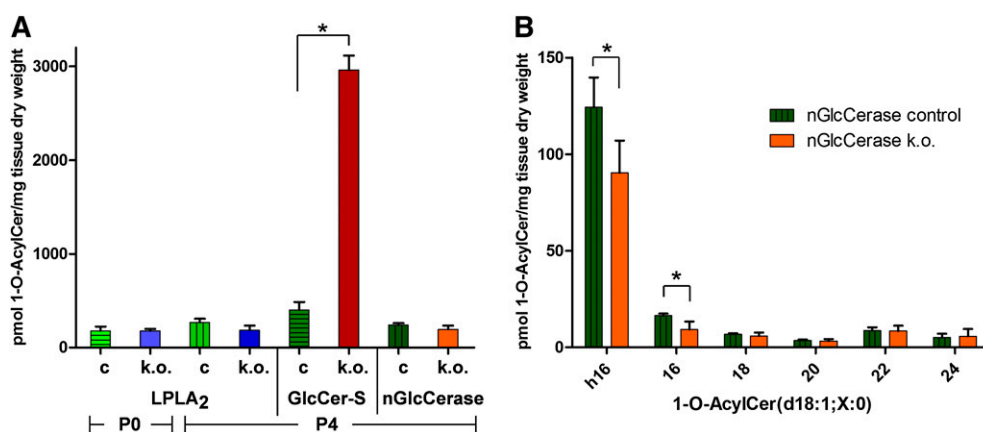

Fig. 5. Quantification of 1-O-acylceramide levels in the epidermis of LPLA$_2$-deficient, keratinocyte-specific GlcCer-S-deficient, nGlcCerase-deficient, and corresponding control mice. A: 1-O-acylceramides containing saturated 1-O-acyl chains from C14 to C26 and parent Cer backbones with either a C17-sphingosine (d17:1) or a C18-sphingosine (d18:1) combined with the N-linked acyl chains hC16:0, C16:0, C18:0, C20:0, C22:0, or C24:0 were quantified by UPLC-MS/MS. 1-O-acylceramide levels were compared between control (c) and the different knockout (k.o.) mice at birth [post natal day (P)0] and 4 days postnatal (P4). The full list of compounds is listed in supplementary Table II. nGlcCerase, neutral glucosylceramidase/Gba2; n = 3 for LPLA$_2$ (P0 and P4), and GlcCer-S control and mutant (k.o.) groups, n = 6 for nGlcCerase controls and n = 4 for nGlcCerase-deficient samples (k.o.). B: Detailed analysis of epidermal 1-O-acylceramides from neutral glucosylceramidase-deficient mice. C18-sphingosines containing 1-O-acylceramides were grouped according to their parent Cer [1-O-acyl Cer(d18:1;X:0)]. Note a significant decrease of those 1-O-acyl Cers containing an N-linked hydroxy-palmitoyl chain (h16; 73% of controls) or an N-linked palmitoyl chain (16; 56% of controls), which nicely corresponds to a simultaneous decrease of these free Cers [Cer(d18:1;h16:0) and Cer(d18:1;16:0)] in neutral glucosylceramidase-deficient mice (supplementary Fig. VI); p < 0.05.

chain Cers (17). We investigated the involvement of LPLA$_2$ in epidermal 1-O-acylceramide synthesis by comparing 1-O-acylceramide levels from extracts of controls and LPLA$_2$ mutants. At the 5% level, no differences were observed at birth or 4 days after birth, excluding a major role of LPLA$_2$ in epidermal 1-O-acylceramide synthesis (Fig. 5 and supplementary Fig. IV).

Loss of neutral glucosylceramidase activity does influence individual 1-O-acylceramide levels

GlcCer is synthesized at the cytosolic side of the *cis*-Golgi (24, 25). Then, it is either used to generate more complex GSLs on the luminal side or it may be degraded back to Cer by neutral glucosylceramidase at the cytosolic side of the Golgi, endoplasmic reticulum (ER), or plasma membrane (26, 27). If neutral glucosylceramidase is located at sites en route to 1-O-acylation of Cers, it could enhance local concentrations of Cers used for 1-O-acylation. Correspondingly, loss of neutral glucosylceramidase then would lead to decreased substrate availability and concomitantly lower 1-O-acylceramide levels. Previously, elevated steady-state GlcCer levels were reported for liver and testis of neutral glucosylceramidase-deficient mice (20, 28, 29), but were also observed in the spleen, kidney, and brain of these mice (unpublished observations). In epidermis, we analyzed GlcCers with a Cer anchor also present in 1-O-acylceramides and observed a 2- to 3-fold increase in mutants. Correspondingly, levels of the more abundant Cers with long (C16-) acyl chains, but not of Cers with the very long (C24-) acyl chains, decreased down to 52% (16:0) and 61% (h16:0) (supplementary Fig. VI). These Cers may be used as substrates for 1-O-acylation. And indeed significantly lower levels of 1-O-acylceramides with *N*-linked C16-acyl chains were observed in neutral glucosylceramidase-deficient epidermis (Fig. 5B). As longer 1-O-acylceramides were not altered, the overall decrease of 1-O-acylceramides (80% as compared with controls) was not significant at the 5% level (Fig. 5A).

1-O-acylceramides are present in human stratum corneum

To investigate whether 1-O-acylceramides also occur in human stratum corneum and/or the surface of human skin, we isolated total lipids from the ventral forearms of three male volunteers by tape stripping. UPLC-coupled tandem mass spectrometric analyses revealed that 1-O-acylceramides are present at 280 ± 70 fmol per pmol of NS-Cers. The latter represent about 7.4% of all Cers in human stratum corneum (30). In humans, 1-O-lignoceroyl Cer(d18:1; h16:0) was the most prominent peak, followed by 1-O-palmitoyl Cer(d18:1;16:0) and 1-O-palmitoyl Cer(d18:1;h16:0) (**Fig. 6**). However, if all parent Cers were summed up, palmitoylation was the most prominent Cer modification in the 1-O-position followed by myristoylation and lignoceroylation (supplementary Fig. VII). The total amount of 1-O-acylceramides accounted for 31 ± 6% of the corresponding unmodified parent Cers.
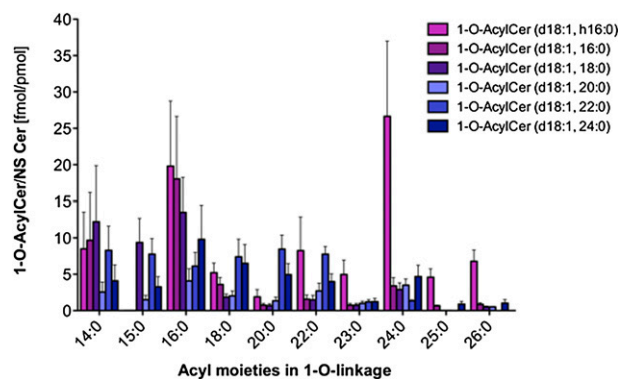

Fig. 6. Quantification of 1-O-acylceramides containing C18-sphingosine in the upper stratum corneum of human skin. Acylceramides (containing a C18-sphingosine) were quantified via UPLC-MS/MS. 1-oleoyl Cer(d18:1;17:0) was used as internal standard. Series refer to the *N*-linked fatty acid of the parent Cer backbones recorded, i.e., h16, Cer(d18:1;h16:0); 16, Cer(d18:1;16:0); 18, Cer(d18:1;18:0); 20, Cer(d18:1;20:0); 22, Cer(d18:1;22:0); and 24, Cer(d18:1;24:0). Note the relative high concentration of 1-O-myristoyl Cers as compared with mouse extracts (supplementary Figs. IV, VII).

DISCUSSION

The formation of 1-O-acylceramides was first observed in rat brain using radioactively labeled substrates (16). In the 1990s, an enzyme with Cer 1-O-acyltransferase activity was identified in MDCK cells and mouse brain, spleen, liver, and kidneys (17). This enzyme (LPLA$_2$) predominantly acts as phospholipase A$_2$. In vitro, LPLA$_2$ has been shown to be most active using short chain Cer (C2-Cer) for 1-O-acylation (17, 18). Recently, a novel Cer 1-O-acylation pathway was discovered in yeast. Here, very long chain Cers (C26-Cer) were 1-O-acylated and the reaction was catalyzed by the diacylglycerol acyltransferases Lro1p and Dga1p (19). Lecithin:cholesterol acyltransferase (LCAT) and LPLA$_2$ are human homologs of the yeast Lro1p. Whereas LCAT and LPLA$_2$ are localized either outside of the cell or within lysosomes, Lro1p acts in the lumen of the ER (19, 31). Also the activity of Dga1p, which is a homolog to the mammalian diacylglycerol O-acyltransferase 2 (DGAT2), is localized in the ER, but it is most prominent in lipid droplets (32–34). Interestingly, mice deficient for DGAT2 exhibit not only lipopenia, but also skin barrier abnormalities (35).

Whereas the previous studies shed light on the biosynthetic pathways of Cer 1-O-acylation in yeast and mammalian cells, an in-depth analysis of the composition of endogenous 1-O-acylceramides and their natural concentrations is missing. Here, we report the complete endogenous structures of almost a hundred 1-O-acylceramides as natural components of murine and human epidermis/stratum corneum. However, combinatorial calculations for mouse epidermis hint to even more (>200) components eventually present in trace amounts.

Epidermis is one of the richest sources for Cers and displays a high Cer structural diversity (8, 9). Van Smeden et al. (9) and Wertz and Downing (36) pointed out the presence of a very hydrophobic series of unknown esterified

Cers, which probably contain a hydroxyl group less than the well-established ω-esterified ultra-long chain Cers (EOS). In the mouse epidermis, we also observed esterified Cers of unknown structures. In keratinocyte-specific GlcCer-synthase-deficient mice (22), the levels of these Cers are strongly increased. These observations suggest that GlcCer-S and 1-O-acyltransferase may compete for the same Cer substrates. These Cers are still present in CerS3-deficient mice, which lack all epidermal Cers with N-acyl chains of 26 or more carbon atoms in length (10). Here, analysis of the lipid extracts from CerS3-deficient mice facilitated the characterization of the unknown esterified Cers as 1-O-acylceramides. Their parent Cer backbones belong to group I of long and very long chain epidermal Cers, which are found in many other tissues. Both the 1-O- and the N-linked acyl chains predominantly found in 1-O-acylceramides are of saturated long to very long chain type, and the sphingoid base is a sphingosine. Hence, only one free hydroxyl group in 3-position of the 1-O-acylceramides remains (except for one series with N-linked hydroxyl-palmitic acid). Therefore, the 1-O-acylceramides that we describe here for mouse epidermis and human stratum corneum/skin surface could represent the earlier described "series A" of unknown esterified Cers in human stratum corneum (9).

The phospholipid-rich plasma membrane of keratinocytes degrades after transformation into corneocytes (37). This process involves the secretion of lysosomal lipases. Hence, during this process 1-O-acylceramides could be produced by lysosomal phospholipases that transfer fatty acids from phospholipids to Cers, which have been secreted by lamellar bodies. Here, we found saturated fatty acids and especially lignoceric acid (C24:0) to be linked to the 1-O-position of Cers in human and mouse epidermis. However, phosphoglycerolipids do not contain substantial amounts of lignoceric acid and usually are rich in unsaturated fatty acids linked to their sn2-position. Hence, it is unlikely that fatty acids esterified to Cers were derived from phosphoglycerolipids. This is further supported by the fact that the bulk of epidermal 1-O-acylceramide synthesis does not depend on LPLA$_2$. In epidermis, 1-O-acylceramide synthesis rather seems to compete with GlcCer synthesis, as a loss of GlcCer synthase leads to a strong increase of 1-O-acylceramides. GlcCer synthase is localized at the cytoplasmic side of the *cis*-Golgi. Hence, Cers that are not converted to GlcCer might be transported back to the ER or to lipid droplets where they could be 1-O-acylated by DGAT2, the homolog of the yeast Dga1p. DGAT2 normally acylates diacylglycerols and resides in lipid droplets. Linoleic acid needed for ω-esterification of ω-hydroxy Cers is derived from triglycerides stored in lipid droplets (38). Furthermore, inducible deficiency of GlcCer-S in keratinocytes also leads to significantly elevated EOS-Cers, which suggests ω-esterification also occurs after Cers have passed the early Golgi apparatus. Therefore, the place of 1-O-acylceramide synthesis could be identical to where ω-hydroxy (glucosyl)ceramides are esterified with linoleic acid in dependence of comparative gene identification-58 [abhydrolase domain containing 5 (ABHD5)] (38), and

might be a lamellar body-lipid droplet contact site. Lamellar bodies finally transport ω-esterified Cers and GlcCers to the interface of stratum granulosum and stratum corneum where they are released to form extracellular lipid lamellae and the cornified lipid envelope (11). However, the cellular origin of epidermal 1-O-acylceramides still has to be established; and sebaceous glands, a rich source of unpolar lipids (39), may not be excluded.

Interestingly, deficiency of the cytosolically oriented neutral glucosylceramidase, which is tightly attached to membranes of the Golgi and the ER (26) or the plasma membrane (27), was accompanied by a decrease of those 1-O-acylceramides for which we also observed a decrease of the corresponding precursor (parent) Cers, suggesting neutral glucosylceramidase activity to be topologically related and upstream of 1-O-acylceramide production.

As pointed out earlier (19), 1-O-acylceramides should not support lipid bilayer formation. However, 1-O-acylceramides are also more polar than triglycerides, wax esters, or cholesterol esters. 1-O-acylceramides contain a free hydroxyl group, which allows them to undergo oriented hydrogen bonding interactions. Due to their predicted physicochemical properties, 1-O-acylceramides might constitute building blocks of extracellular lipid lamellae and may contribute to their stability and correct lamella phase organization. Lamella phase organization has been shown to be disturbed in patients with atopic eczema (40). In spite of their relatively low abundance (5% of all esterified Cers, or 2.3% of all Cers, which account roughly for about half of the total stratum corneum lipid species by weight) (41). 1-O-acylceramides could contribute to a functional water permeability barrier as they are among the most hydrophobic epidermal Cers. However, this has to be clarified in future investigations.⬛

REFERENCES

1. Mullen, T. D., Y. A. Hannun, and L. M. Obeid. 2012. Ceramide synthases at the centre of sphingolipid metabolism and biology. *Biochem. J.* **441:** 789–802.
2. Hannun, Y. A., and L. M. Obeid. 2008. Principles of bioactive lipid signalling: lessons from sphingolipids. *Nat. Rev. Mol. Cell Biol.* **9:** 139–150.
3. Zhang, H., N. N. Desai, A. Olivera, T. Seki, G. Brooker, and S. Spiegel. 1991. Sphingosine-1-phosphate, a novel lipid, involved in cellular proliferation. *J. Cell Biol.* **114:** 155–167.
4. Kolter, T., and K. Sandhoff. 1999. Sphingolipids - their metabolic pathways and the pathobiochemistry of neurodegenerative diseases. *Angew. Chem. Int. Ed. Engl.* **38:** 1532–1568.
5. Gómez-Muñoz, A. 2006. Ceramide 1-phosphate/ceramide, a switch between life and death. *Biochim. Biophys. Acta.* **1758:** 2049–2056.
6. Lamour, N. F., and C. E. Chalfant. 2005. Ceramide-1-phosphate: the "missing" link in eicosanoid biosynthesis and inflammation. *Mol. Interv.* **5:** 358–367.
7. Subramanian, P., R. V. Stahelin, Z. Szulc, A. Bielawska, W. Cho, and C. E. Chalfant. 2005. Ceramide 1-phosphate acts as a positive allosteric activator of group IVA cytosolic phospholipase A2 alpha and

enhances the interaction of the enzyme with phosphatidylcholine. *J. Biol. Chem.* **280:** 17601–17607.

8. Masukawa, Y., H. Narita, E. Shimizu, N. Kondo, Y. Sugai, T. Oba, R. Homma, J. Ishikawa, Y. Takagi, T. Kitahara, et al. 2008. Characterization of overall ceramide species in human stratum corneum. *J. Lipid Res.* **49:** 1466–1476.

9. van Smeden, J., L. Hoppel, R. van der Heijden, T. Hankemeier, R. J. Vreeken, and J. A. Bouwstra. 2011. LC/MS analysis of stratum corneum lipids: ceramide profiling and discovery. *J. Lipid Res.* **52:** 1211–1221.

10. Jennemann, R., M. Rabionet, K. Gorgas, S. Epstein, A. Dalpke, U. Rothermel, A. Bayerle, F. van der Hoeven, S. Imgrund, J. Kirsch, et al. 2012. Loss of ceramide synthase 3 causes lethal skin barrier disruption. *Hum. Mol. Genet.* **21:** 586–608.

11. Sandhoff, R. 2010. Very long chain sphingolipids: tissue expression, function and synthesis. *FEBS Lett.* **584:** 1907–1913.

12. Rabionet, M., K. Gorgas, and R. Sandhoff. 2013. Ceramide synthesis in the epidermis. *Biochim. Biophys. Acta.* Epub ahead of print. August 27, 2013; doi:10.1016/j.bbalip.2013.08.011.

13. Breiden, B., and K. Sandhoff. 2013. The role of sphingolipid metabolism in cutaneous permeability barrier formation. *Biochim. Biophys. Acta.* Epub ahead of print. August 15, 2013; doi:10.1016/j.bbalip.2013.08.010.

14. Uchida, Y. 2011. The role of fatty acid elongation in epidermal structure and function. *Dermatoendocrinol.* **3:** 65–69.

15. Uchida, Y., and W. M. Holleran. 2008. Omega-O-acylceramide, a lipid essential for mammalian survival. *J. Dermatol. Sci.* **51:** 77–87.

16. Okabe, H., and Y. Kishimoto. 1977. In vivo metabolism of ceramides in rat brain. Fatty acid replacement and esterification of ceramide. *J. Biol. Chem.* **252:** 7068–7073.

17. Abe, A., J. A. Shayman, and N. S. Radin. 1996. A novel enzyme that catalyzes the esterification of N-acetylsphingosine. Metabolism of C2-ceramides. *J. Biol. Chem.* **271:** 14383–14389.

18. Shayman, J. A., R. Kelly, J. Kollmeyer, Y. Q. He, and A. Abe. 2011. Group XV phospholipase A$_2$, a lysosomal phospholipase A$_2$. *Prog. Lipid Res.* **50:** 1–13.

19. Voynova, N. S., C. Vionnet, C. S. Ejsing, and A. Conzelmann. 2012. A novel pathway of ceramide metabolism in Saccharomyces cerevisiae. *Biochem. J.* **447:** 103–114.

20. Yildiz, Y., H. Matern, B. Thompson, J. C. Allegood, R. L. Warren, D. M. Ramirez, R. E. Hammer, F. K. Hamra, S. Matern, and D. W. Russell. 2006. Mutation of beta-glucosidase 2 causes glycolipid storage disease and impaired male fertility. *J. Clin. Invest.* **116:** 2985–2994.

21. Hiraoka, M., A. Abe, Y. Lu, K. Yang, X. Han, R. W. Gross, and J. A. Shayman. 2006. Lysosomal phospholipase A2 and phospholipidosis. *Mol. Cell. Biol.* **26:** 6139–6148.

22. Jennemann, R., R. Sandhoff, L. Langbein, S. Kaden, U. Rothermel, H. Gallala, K. Sandhoff, H. Wiegandt, and H. J. Gröne. 2007. Integrity and barrier function of the epidermis critically depend on glucosylceramide synthesis. *J. Biol. Chem.* **282:** 3083–3094.

23. Jennemann, R., S. Kaden, R. Sandhoff, V. Nordström, S. Wang, M. Volz, S. Robine, N. Amen, U. Rothermel, H. Wiegandt, et al. 2012. Glycosphingolipids are essential for intestinal endocytic function. *J. Biol. Chem.* **287:** 32598–32616.

24. Jeckel, D., A. Karrenbauer, K. N. Burger, G. van Meer, and F. Wieland. 1992. Glucosylceramide is synthesized at the cytosolic surface of various Golgi subfractions. *J. Cell Biol.* **117:** 259–267.

25. Futerman, A. H., and R. E. Pagano. 1991. Determination of the intracellular sites and topology of glucosylceramide synthesis in rat liver. *Biochem. J.* **280:** 295–302.

26. Körschen, H. G., Y. Yildiz, D. N. Raju, S. Schonauer, W. Bönigk, V. Jansen, E. Kremmer, U. B. Kaupp, and D. Wachten. 2013. The non-lysosomal β-glucosidase GBA2 is a non-integral membrane-associated protein at the endoplasmic reticulum (ER) and Golgi. *J. Biol. Chem.* **288:** 3381–3393.

27. Aureli, M., R. Bassi, N. Loberto, S. Regis, A. Prinetti, V. Chigorno, J. M. Aerts, R. G. Boot, M. Filocamo, and S. Sonnino. 2012. Cell surface associated glycohydrolases in normal and Gaucher disease fibroblasts. *J. Inherit. Metab. Dis.* **35:** 1081–1091.

28. Walden, C. M., R. Sandhoff, C. C. Chuang, Y. Yildiz, T. D. Butters, R. A. Dwek, F. M. Platt, and A. C. van der Spoel. 2007. Accumulation of glucosylceramide in murine testis, caused by inhibition of beta-glucosidase 2: implications for spermatogenesis. *J. Biol. Chem.* **282:** 32655–32664.

29. Gonzalez-Carmona, M. A., R. Sandhoff, F. Tacke, A. Vogt, S. Weber, A. E. Canbay, G. Rogler, T. Sauerbruch, F. Lammert, and Y. Yildiz. 2012. Beta-glucosidase 2 knockout mice with increased glucosylceramide show impaired liver regeneration. *Liver Int.* **32:** 1354–1362.

30. t'Kindt, R., L. Jorge, E. Dumont, P. Couturon, F. David, P. Sandra, and K. Sandra. 2012. Profiling and characterizing skin ceramides using reversed-phase liquid chromatography-quadrupole time-of-flight mass spectrometry. *Anal. Chem.* **84:** 403–411.

31. Choudhary, V., N. Jacquier, and R. Schneiter. 2011. The topology of the triacylglycerol synthesizing enzyme Lro1 indicates that neutral lipids can be produced within the luminal compartment of the endoplasmatic reticulum: Implications for the biogenesis of lipid droplets. *Commun. Integr. Biol.* **4:** 781–784.

32. Jacquier, N., V. Choudhary, M. Mari, A. Toulmay, F. Reggiori, and R. Schneiter. 2011. Lipid droplets are functionally connected to the endoplasmic reticulum in Saccharomyces cerevisiae. *J. Cell Sci.* **124:** 2424–2437.

33. Natter, K, P. Leitner, A. Faschinger, H. Wolinski, S. McCraith, S. Fields, and S. D. Kohlwein. 2005. The spatial organization of lipid synthesis in the yeast Saccharomyces cerevisiae derived from large scale green fluorescent protein tagging and high resolution microscopy. *Mol. Cell. Proteomics.* **4:** 662–672.

34. Sorger, D., and G. Daum. 2002. Synthesis of triacylglycerols by the acyl-coenzyme A:diacyl-glycerol acyltransferase Dga1p in lipid particles of the yeast Saccharomyces cerevisiae. *J. Bacteriol.* **184:** 519–524.

35. Stone, S. J., H. M. Myers, S. M. Watkins, B. E. Brown, K. R. Feingold, P. M. Elias, and R. V. Farese, Jr. 2004. Lipopenia and skin barrier abnormalities in DGAT2-deficient mice. *J. Biol. Chem.* **279:** 11767–11776.

36. Wertz, P. W., and D. T. Downing. 1983. Ceramides of pig epidermis: structure determination. *J. Lipid Res.* **24:** 759–765.

37. Mao-Qiang, M., K. R. Feingold, M. Jain, and P. M. Elias. 1995. Extracellular processing of phospholipids is required for permeability barrier homeostasis. *J. Lipid Res.* **36:** 1925–1935.

38. Radner, F. P., I. E. Streith, G. Schoiswohl, M. Schweiger, M. Kumari, T. O. Eichmann, G. Rechberger, H. C. Koefeler, S. Eder, S. Schauer, et al. 2010. Growth retardation, impaired triacylglycerol catabolism, hepatic steatosis, and lethal skin barrier defect in mice lacking comparative gene identification-58 (CGI-58). *J. Biol. Chem.* **285:** 7300–7311.

39. Picardo, M., M. Ottaviani, E. Camera, and A. Mastrofrancesco. 2009. Sebaceous gland lipids. *Dermatoendocrinol.* **1:** 68–71.

40. Janssens, M., J. van Smeden, G. S. Gooris, W. Bras, G. Portale, P. J. Caspers, R. J. Vreeken, S. Kezic, A. P. Lavrijsen, and J. A. Bouwstra. 2011. Lamellar lipid organization and ceramide composition in the stratum corneum of patients with atopic eczema. *J. Invest. Dermatol.* **131:** 2136–2138.

41. Holleran, W. M., Y. Takagi, and Y. Uchida. 2006. Epidermal sphingolipids: metabolism, function, and roles in skin disorders. *FEBS Lett.* **580:** 5456–5466.